SAND2017-8581C

Exceptional service in the national interest

Sandia National Laboratories

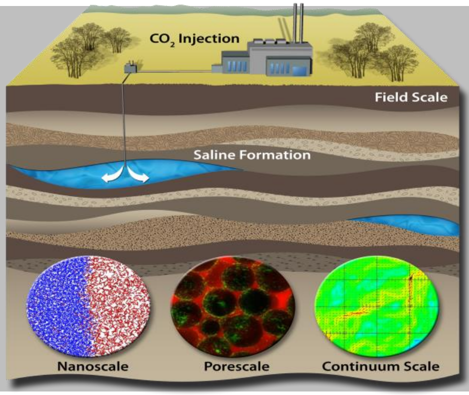

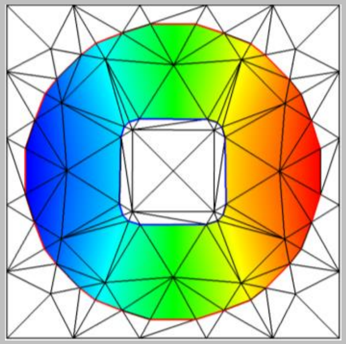

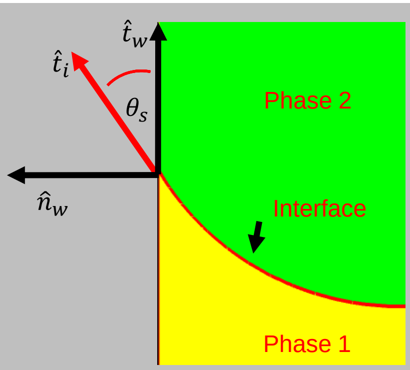

A Conformal Decomposition Finite Element Method for Dynamic Wetting Applications

David R. Noble, Alec Kucala, and
Mario J. Martinez

U.S. DEPARTMENT OF ENERGY NNSA National Nuclear Security Administration

Sandia National Laboratories is a multimission laboratory managed and operated by National Technology and Engineering Solutions of Sandia, LLC, a wholly owned subsidiary of Honeywell International, Inc., for the U.S. Department of Energy's National Nuclear Security Administration under contract DE-NA0003525.

Motivation

- Injection of CO_2 into reservoir rocks is a strategy of reducing greenhouse gas emissions
- Modeling CO_2 migration and capillary trapping at the pore scale is important in predicting the permeability characteristics of reservoir rocks
  - Hydrophobicity or hydrophilicity of the reservoir rock can influence contact line dynamics
- Use computational fluid dynamics to model the multi-phase flow through heterogeneous reservoir rock pores
  - Conformal decomposition finite-element method (CDFEM)
  - Dynamic contact line modeling
- Can be applied to other surface tension dominated flows

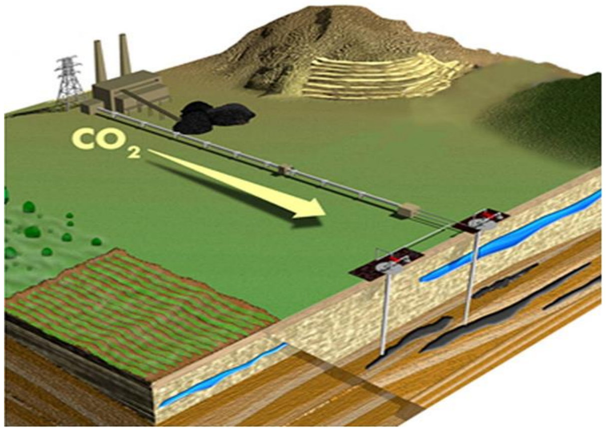

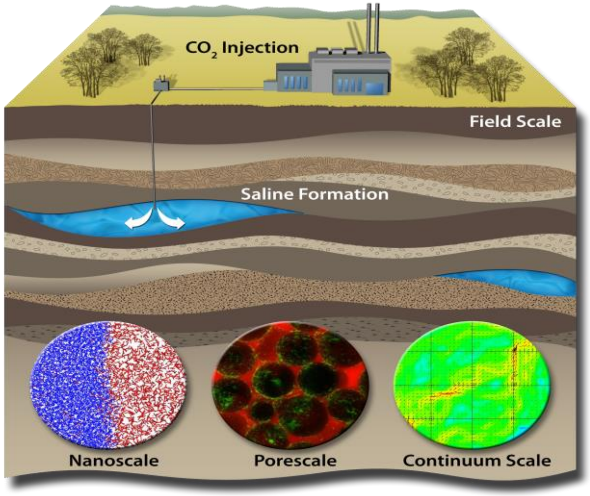

Overview of contact line models

- Two immiscible fluids in contact with a solid surface in equilibrium form a static contact angle
- When this equilibrium is disturbed, the contact angle becomes dynamic and the contact line moves
- Must model relationship between contact angle and contact line velocity as the physics are poorly understood

Hydrodynamic Models

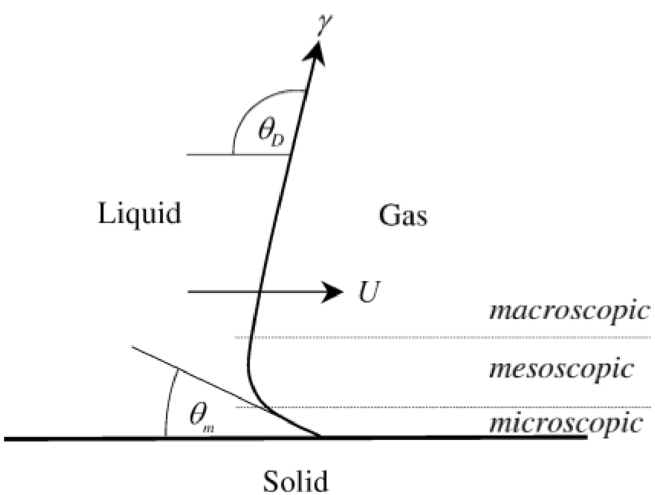

(Blake, 2006)

Molecular Models

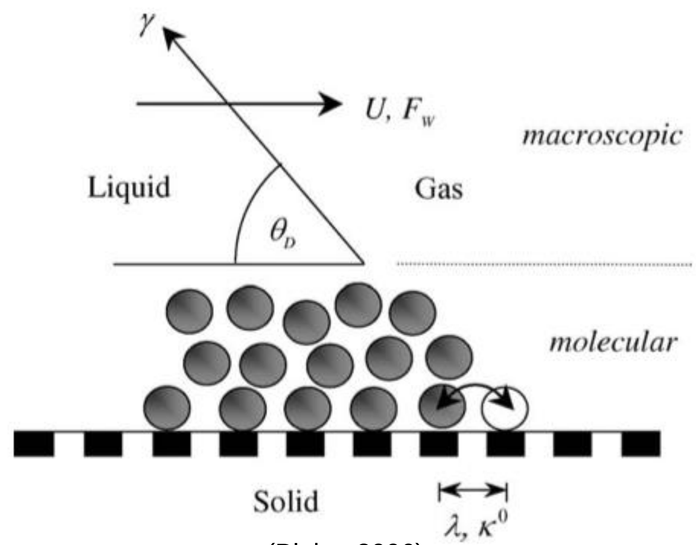

(Blake, 2006)

Hydrodynamic and molecular models

Hydrodynamic Models

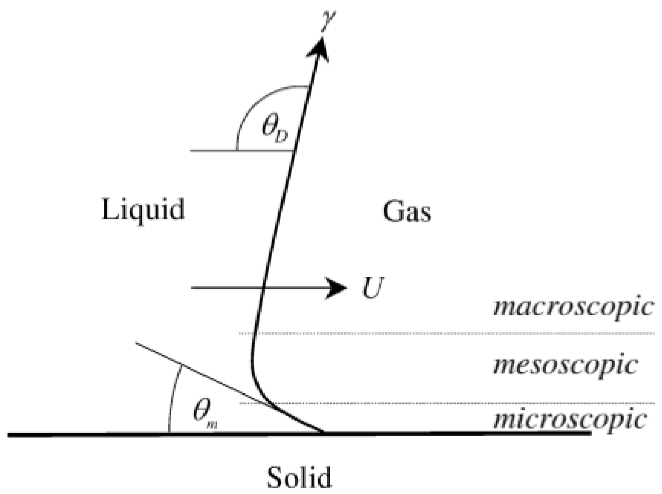

(Blake, 2006)

- Three length scales near the contact line: macroscopic, mesoscopic, and microscopic
- Changes in experimentally observed macroscopic dynamic contact angle is attributed to viscous bending of the interface in the mesoscopic region
- Microscopic angle is usually assumed as the static angle and velocity independent
- Voinov, 1976; Cox, 1989; Huh & Scriven, 1971.

Molecular Models

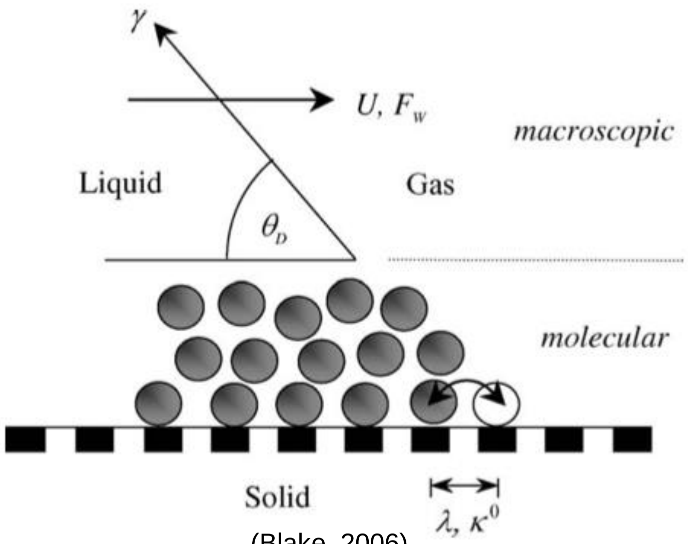

(Blake, 2006)

- Two length scales: macroscopic and molecular
- Contact line motion is determined by the statistical dynamics of the molecules at the molecular scale
- Driving force of contact line is proportional to the disturbed and equilibrium contact angles.
- Blake, 1969

Conformal Decomposition Finite Element Method (CDFEM)

- Simple Concept (Noble, et al. 2010)
  - Use one or more level set fields to define materials or phases
  - Decompose non-conformal elements into conformal ones
  - Obtain solutions on conformal elements
  - Use single-valued fields for weak discontinuities and double-valued fields for strong discontinuities
- Capability Properties
  - Supports wide variety of interfacial conditions (identical to boundary fitted mesh)
  - Avoids manual generation of boundary fitted mesh
  - Supports general topological evolution (subject to mesh resolution)
- Implementation Properties
  - Similar to finite element adaptivity
  - Uses standard finite element assembly including data structures, interpolation, quadrature

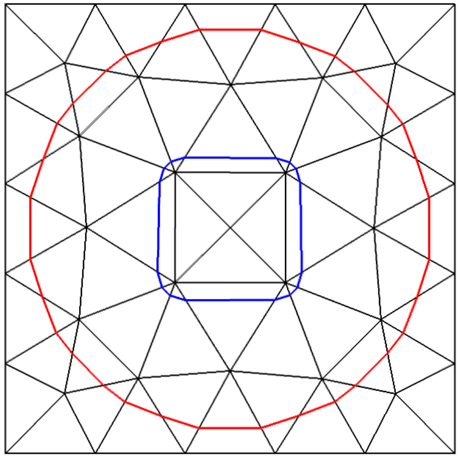

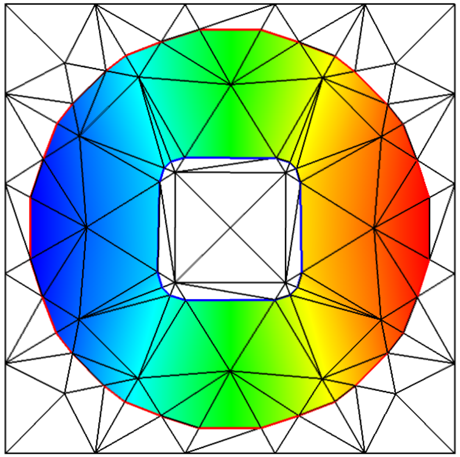

XFEM - CDFEM Code Requirements Comparison

	XFEM	CDFEM
Volume Assembly	Conformal subelement integration, specialized element loops to use modified integration rules	Standard Volume Integration
Surface Flux Assembly	Specialized volume element loops with specialized quadrature	Standard Surface Integration
Phase Specific DOFs and Equations	Different variables present at different nodes of the same block	Block has homogenous dofs/equations
Dynamic DOFS and Equations	Require reinitializing linear system	Require reinitializing linear system
Various BC types on Interface	Dirichlet BCs normally cannot be strongly enforced	Standard Techniques available

CDFEM Applied to Multiphase Flows

- CDFEM used to provide dynamic discretization for multiphase flow with interfaces that do not conform to static finite element meshes
- Level set that advects with the flow is used to define the interface locations
- Adds degrees of freedom (velocity and pressure) by adding nodes to mesh which lie on the exact interface location
- Can apply boundary conditions directly at interface
  - Surface tension
  - Wetting line models

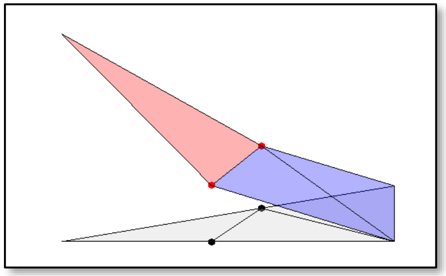

Weakly discontinuous velocity

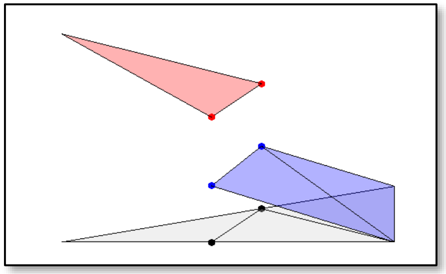

Strongly discontinuous pressure

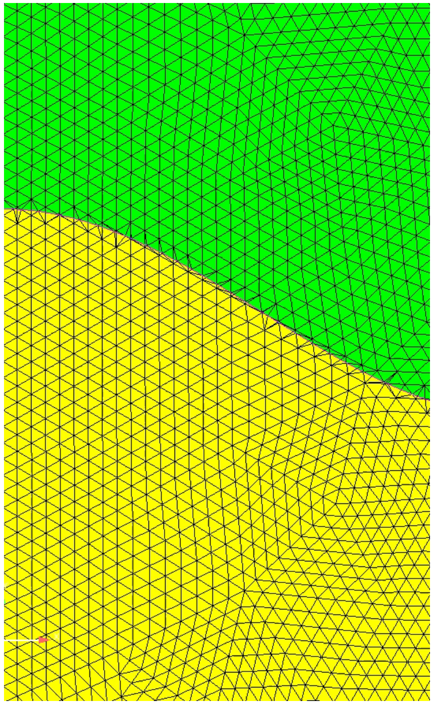

Computational model

- Utilize Galerkin triangular and tetrahedral finite elements to discretize Navier-Stokes equation
- Solved using Sierra multi-physics suite at SNL[1]

Navier-Stokes Equations

$$\nabla \cdot \mathbf{u} = 0$$

$$\rho(\mathbf{x}) \left(\frac{\partial \mathbf{u}}{\partial t} + (\mathbf{u} \cdot \nabla)\, \mathbf{u} \right) = -\nabla p + \nabla \cdot \left(\mu(\mathbf{x}) \left(\nabla \mathbf{u} + \nabla \mathbf{u}^{\mathrm{T}} \right) \right)$$

Level Set Equation

$$\frac{\partial \phi}{\partial t} + \mathbf{u} \cdot \nabla \phi = 0$$

Interface Boundary Conditions

$$[\mathbf{u}]_{\Delta} = 0, \qquad \mathbf{x} \in \Gamma$$ ***(impermeability)***

$$\left[-p\mathbf{I} + \mu(\mathbf{x}) \left(\nabla \mathbf{u} + \nabla \mathbf{u}^{\mathrm{T}} \right) \right]_{\Delta} \cdot \hat{\mathbf{n}} = -\gamma \kappa \hat{\mathbf{n}}, \qquad \mathbf{x} \in \Gamma$$ ***(surface tension)***

1. P. Notz, S. R. Subia, M. M. Hopkins, H. K. Moffat, and D. R. Noble, Aria 1.5: User Manual, SAND2007-2734 (Sandia National Laboratories, Albuquerque, NM, 2007)

Time-discretization scheme (2nd Order)

Momentum Prediction

$$\int_{\Omega^n} (\nabla \cdot \tilde{\mathbf{u}})\, w_i \mathrm{d}\Omega = 0,$$

$$\int_{\Omega^n} \rho \left(\frac{\frac{3}{2}\tilde{\mathbf{u}} - 2\mathbf{u}^n + \frac{1}{2}\mathbf{u}^{n-1}}{\Delta t} + (\tilde{\mathbf{u}} \cdot \nabla)\, \tilde{\mathbf{u}} \right) \cdot \mathbf{w}_i \mathrm{d}\Omega$$
$$+ \int_{\Omega^n} -P\mathbf{I} + \mu \left(\nabla \tilde{\mathbf{u}} + \nabla \tilde{\mathbf{u}}^t \right) \cdot \nabla \mathbf{w}_i \mathrm{d}\Omega$$
$$+ \int_{\Gamma_f^n} \sigma \left((\mathbf{I} - \mathbf{nn}) + \Delta t \underline{\nabla} \tilde{\mathbf{u}} \right) \cdot \nabla \mathbf{w}_i \mathrm{d}\Gamma = 0,$$

Levelset Advection

$$\int_{\Omega^n} \left(\frac{\frac{3}{2}\phi^{n+1} - 2\phi^n + \frac{1}{2}\phi^{n-1}}{\Delta t} + \tilde{\mathbf{u}} \cdot \nabla \phi^{n+1} \right) w_i \mathrm{d}\Omega = 0$$

Conformal Decomposition

- Decompose mesh to conform to updated level set
- Compute mesh “velocity”

Momentum Correction

$$\int_{\Omega^{n+1}} \left(\nabla \cdot \mathbf{u}^{n+1} \right) w_i \mathrm{d}\Omega = 0,$$

$$\int_{\Omega^{n+1}} \rho \left(\frac{\frac{3}{2}\mathbf{u}^{n+1} - 2\mathbf{u}^n + \frac{1}{2}\mathbf{u}^{n-1}}{\Delta t} + \left(\left(\mathbf{u}^{n+1} - \dot{\mathbf{x}} \right) \cdot \nabla \right) \mathbf{u}^{n+1} \right) \cdot \mathbf{w}_i \mathrm{d}\Omega$$
$$+ \int_{\Omega^{n+1}} -P\mathbf{I} + \mu \left(\nabla \mathbf{u} + \nabla \mathbf{u}^t \right)^{n+1} \cdot \nabla \mathbf{w}_i \mathrm{d}\Omega$$
$$+ \int_{\Gamma_f^{n+1}} \sigma \left((\mathbf{I} - \mathbf{nn}) + \Delta t \underline{\nabla} \left(\mathbf{u}^{n+1} - \tilde{\mathbf{u}} \right) \right) \cdot \nabla \mathbf{w}_i \mathrm{d}\Gamma = 0,$$

Verification and validation (capillary wave decay)

- Perturb two-phase interface with sinusoidal disturbance
- Interface shape should decay with specific frequency and rate (Prosperetti, 1981) at small amplitudes
- Accurate prediction of capillary wave frequency and amplitude decay
- CDFEM discretization of interface accurately captures surface tension dynamics
- 2^{nd} order convergence in space and time

Interface Dynamics

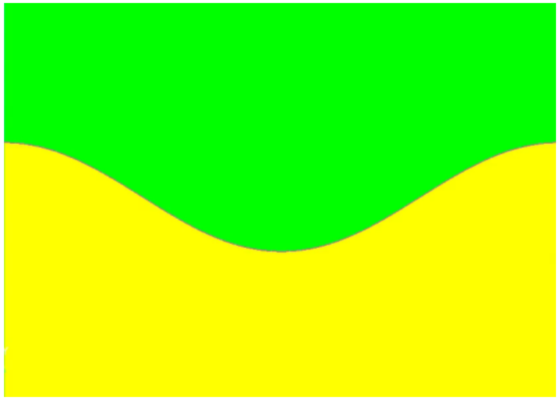

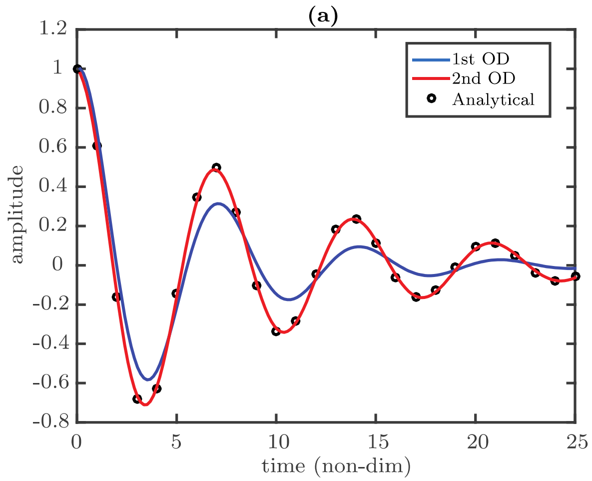

Convergence

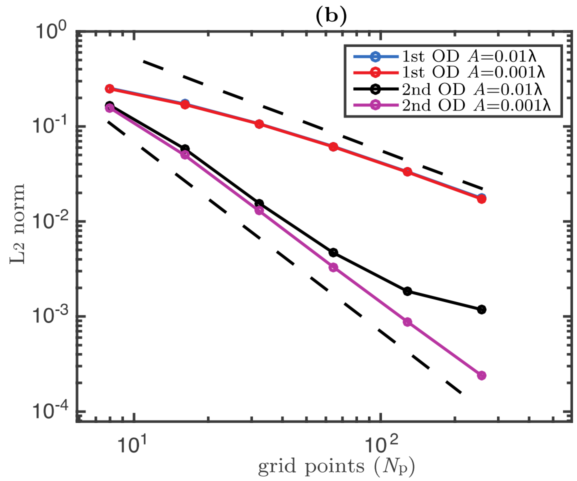

Moving contact line model

Wetting Line Force

$$\vec{f} = \gamma \hat{\tau}_i$$

$$\hat{\tau}_i = \hat{\tau}_w \cos\theta_s + \hat{n}_w \sin\theta_s$$

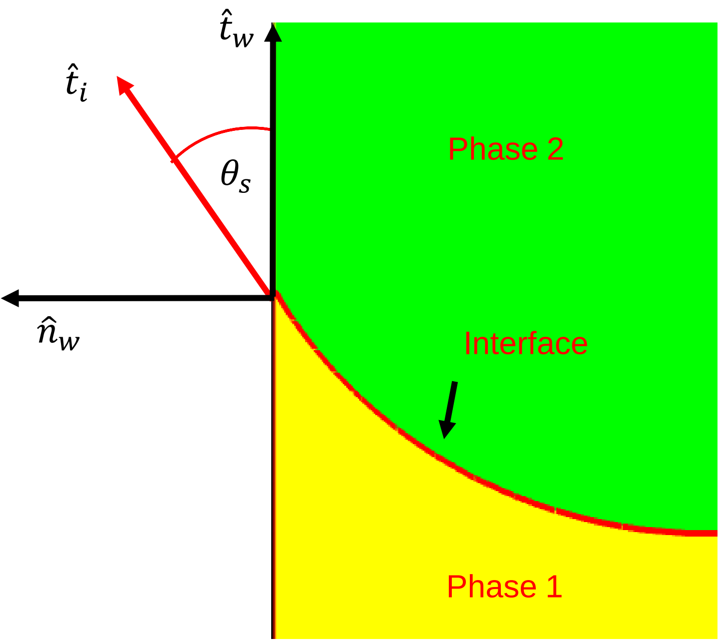

Navier-Slip Condition

$$\vec{f} = \frac{\mu}{\beta}(\vec{v}_w - \vec{v}_{CL})$$

$$Flux = \int \vec{n} \cdot \vec{f} \phi^i \mathrm{d}S$$

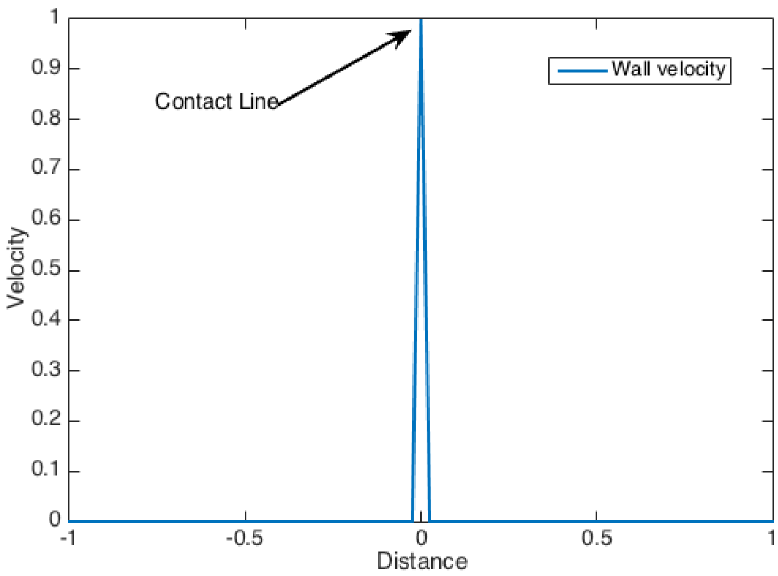

- Assume microscopic (static) contact angle is a constant (θ_s) (hydrodynamic type method)
- For a given fluid pair, specify material properties, surface tension force (γ), and static contact angle (θ_s)
- Pull contact line with surface tension force at Young's equilibrium contact angle
- Select the Navier-Slip length (β) to fit to experimental data

Verification and validation (capillary injection)

Interface Dynamics

Ca = 5.2e-3 (low)   Ca = 4.4e-2 (high)

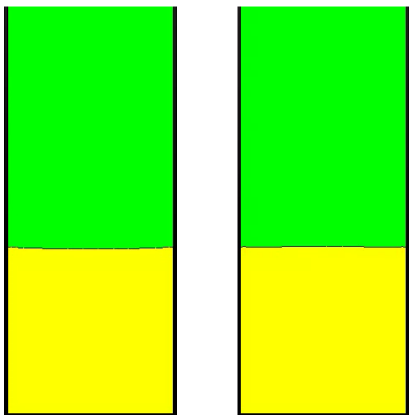

Sancitizer 405 ($\theta_s = 67°$)

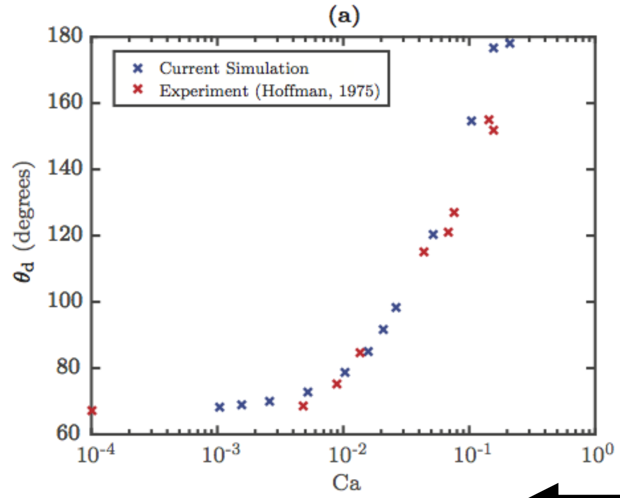

Amdex 760 ($\theta_s = 69°$)

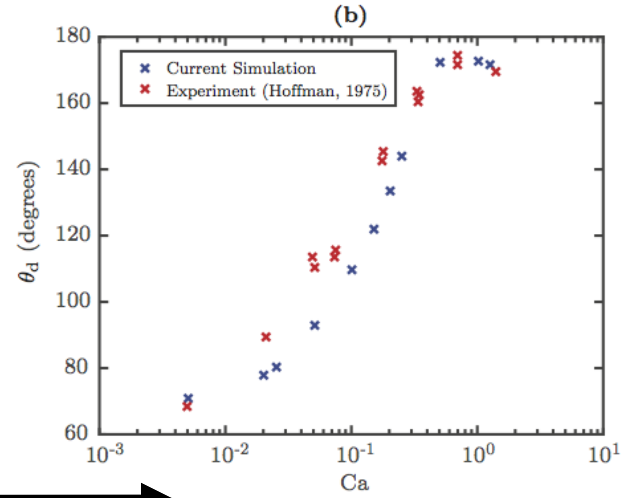

$\beta = 4 \times 10^{-8}$ m

- Injection of fluid into capillary changes dynamic contact angle
- Demonstrate ability to capture dynamic contact angle dependency on capillary number
- Once data is fitted to experiment (one point), specified slip length β becomes independent of fluid type and capillary number

Verification and validation (capillary injection cont.)

Mesh Dependency

MESH DEPENDENT

$\beta = 4.0 \times 10^{-8} = \text{constant}$

MESH INDEPENDENT

$\Delta x/\beta = \text{constant}$

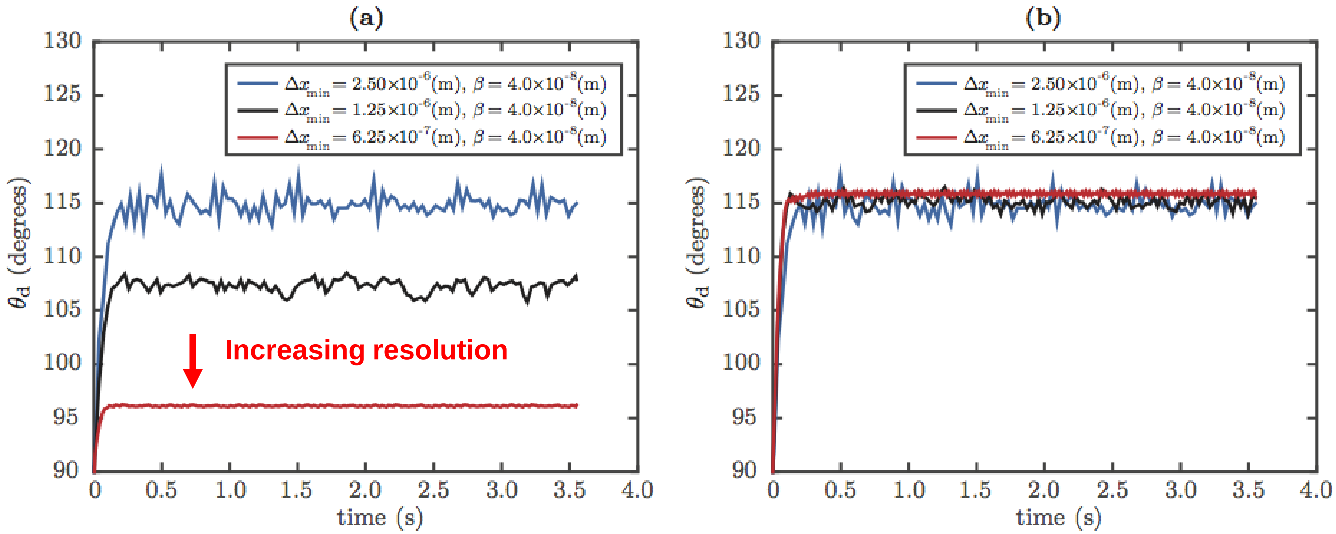

$$\text{Ca} = 4.4 \times 10^{-2}$$

- Solution exhibits mesh dependency (slip length must be adjusted to accommodate resolution changes)
- Mesh independency alleviated once ratio between grid resolution and slip length is held constant
- Allows the use of this model for other more complicated geometries where mesh size is not known *a priori* after slip coefficient is fitted to simple experimental data.

Verification and validation (capillary rise)

2D Capillary Rise

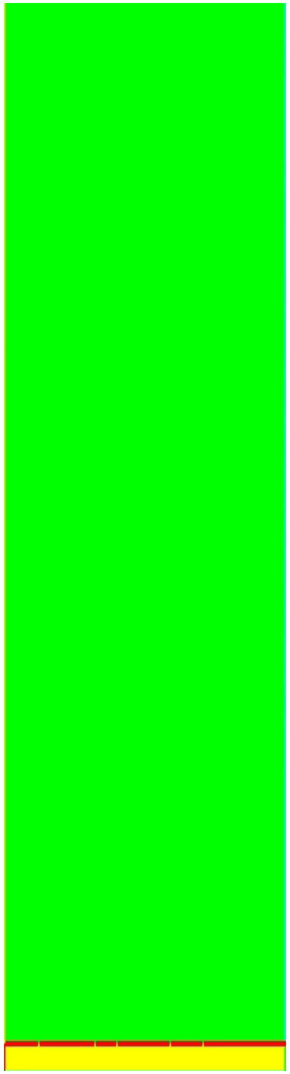

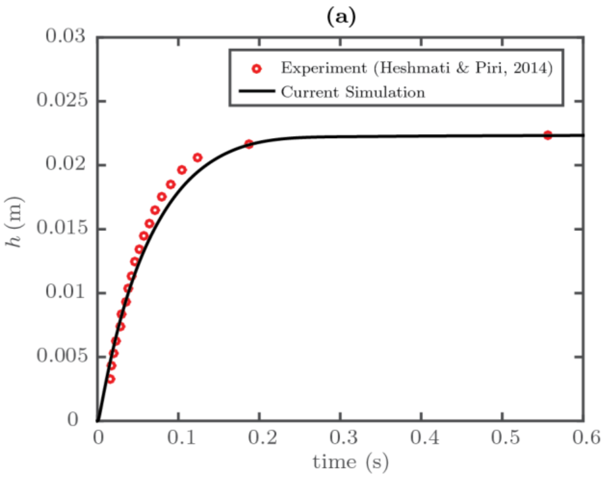

Rise height vs. time

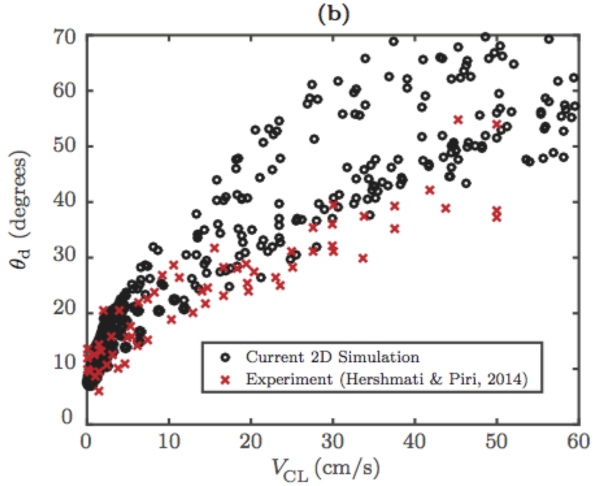

Dynamic angle vs. CL velocity

3D Interface Shapes

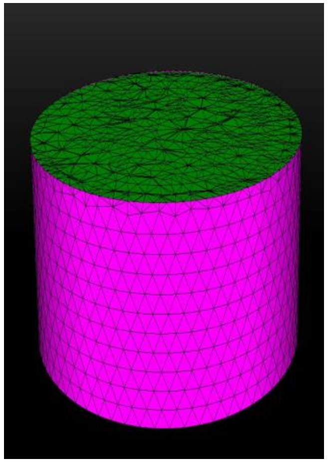

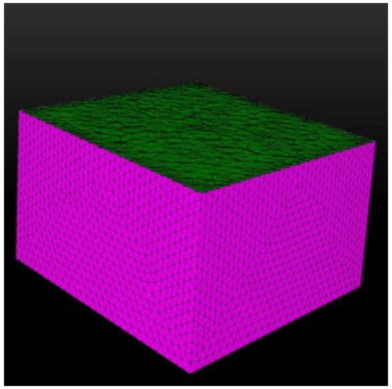

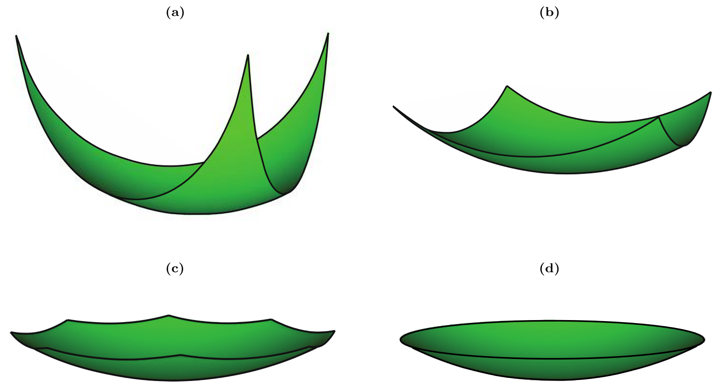

Flow through pore network

Flow Through a Pore Network

Imbibition

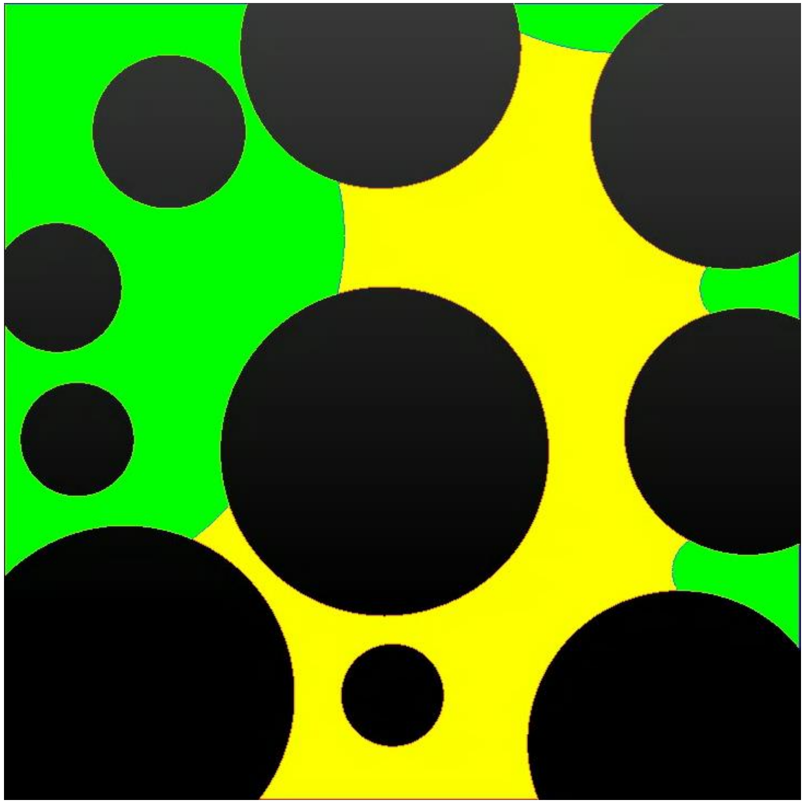

Drainage

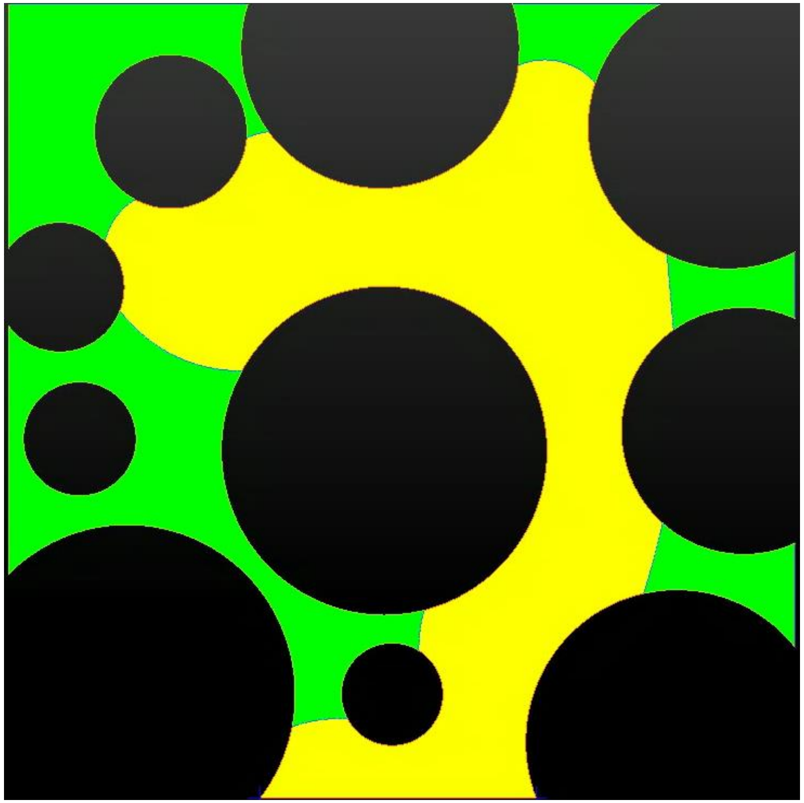

Flow through a scan of a real 3D fracture

- Micro-CT scan of real sandstone fracture
- Mesh generation using CDFEM
- Run multiphase flow on mesh

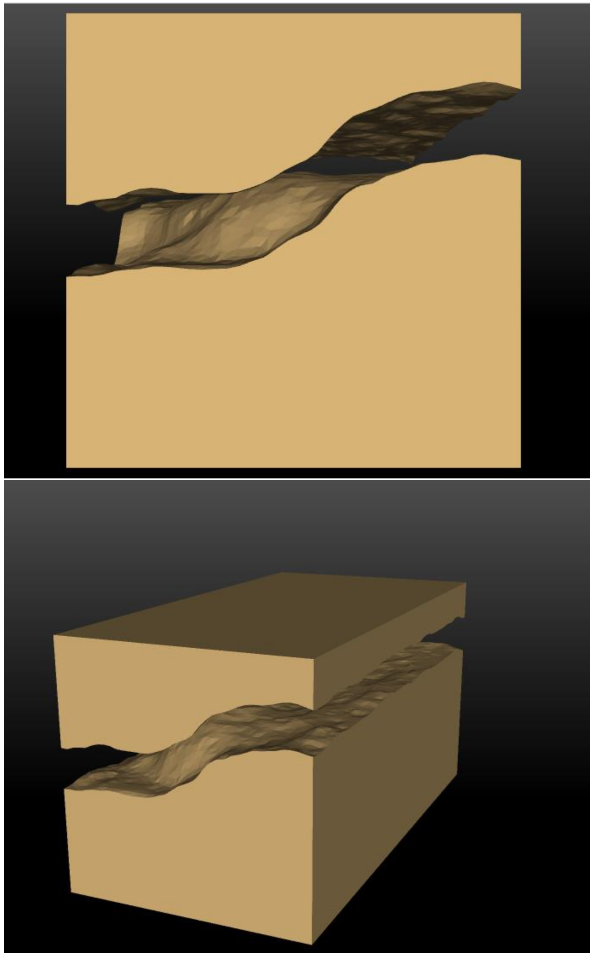

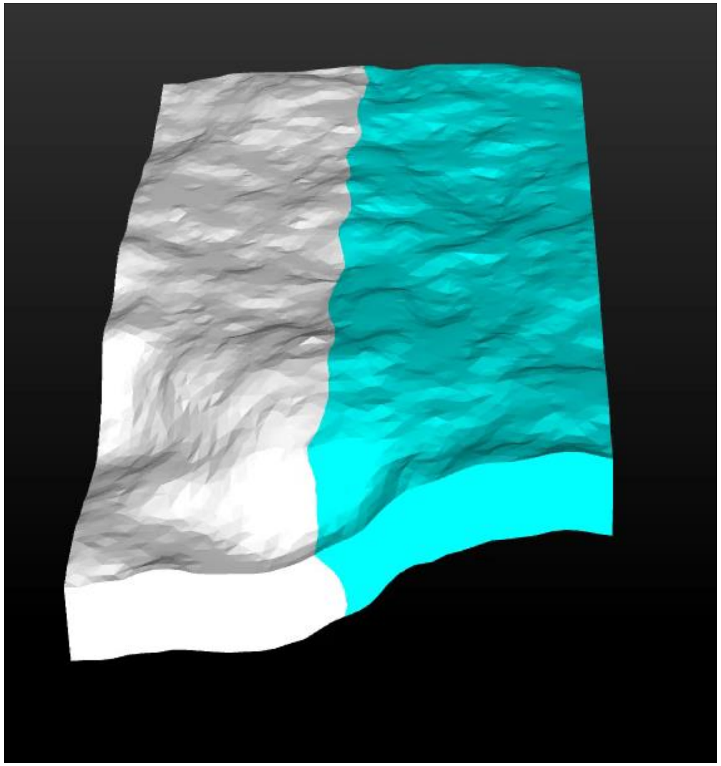

Conclusions

- CDFEM for Multiphase Flows
  - Sharp interface method
    - Captures interfacial discontinuities sharply
    - Allows for sharp wetting line models
  - CDFEM design encapsulates interface motion/discretization and finite element assembly/physics
    - Enriched finite element without rewriting code
  - Verified 2nd order accurate predictor-corrector semi-implicit algorithm
- Wetting line model
  - Single parameter model captures physics over range of static angles and capillary numbers
- Future work
  - Flow in complex, reconstructed pore networks

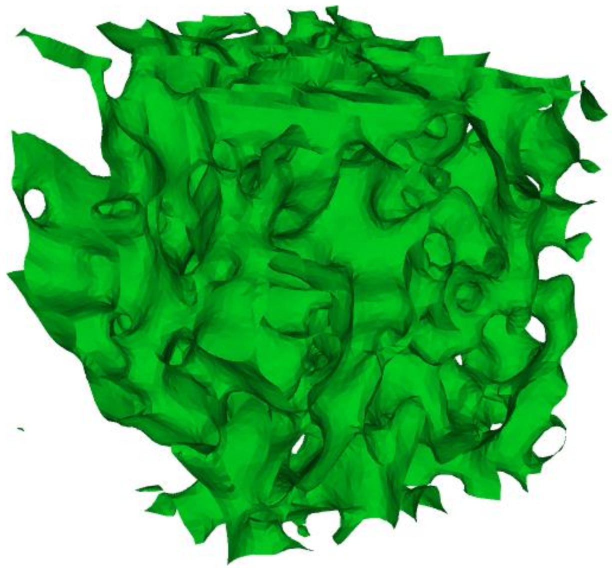

3D micro CT scan of sandstone sample

Impact of Mesh Quality

Three Criteria for Linear Elements

Let f be a function.
Let g be a piecewise linear interpolant of f over some triangulation.

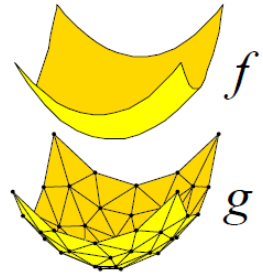

Criterion	
Interpolation error $\|\| f - g \|\|_\infty$	Size very important. Shape only marginally important.
Gradient interpolation error $\|\| \nabla f - \nabla g \|\|_\infty$	Size important. Large angles bad; small okay. 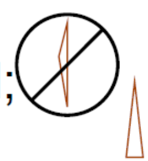
Element stiffness matrix maximum eigenvalue λ_{max}	Small angles bad; large okay. 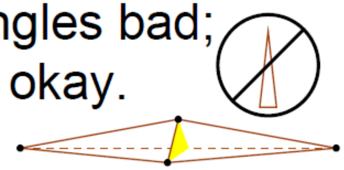

Reprinted from “What is a Good Finite Element?” by Jonathan Richard Shewchuk

Static Interface CDFEM Verification

- Steady Potential Flow about a Sphere
  - Embedded curved boundaries
  - Dirichlet BC on outer surface, Natural BC on inner surface
  - Optimal convergence rates for solution and gradient both on volume and b

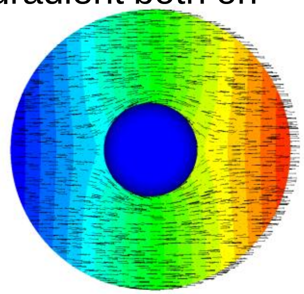

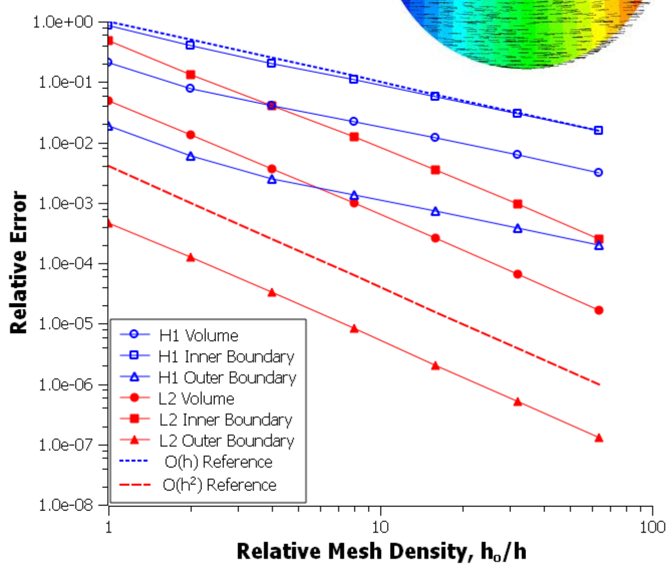

- Steady, Viscous Flow about a Periodic Array of Spheres
  - Embedded curved boundaries
  - Dirichlet BC on sphere surface
  - Accurate results right up to close packing limit
  - Sum of nodal residuals provides accurate/convergent measure of drag force

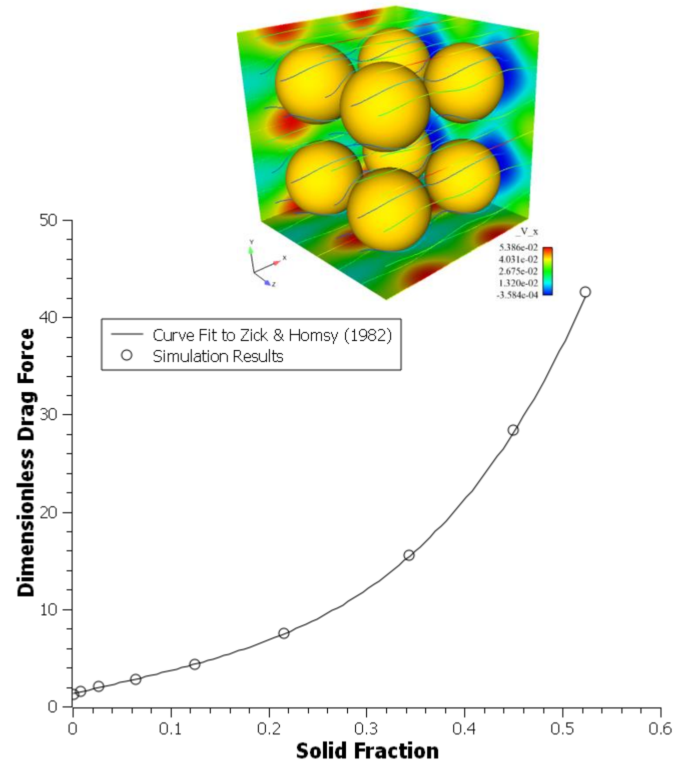

Approach for Dynamic Discretizations: Moving Mesh (MM)

- Uses Arbitrary Lagrangian Eulerian (ALE) technology for moving meshes
  - Relates time derivative following a moving point to the time derivative fixed in space

$$\left.\frac{\partial \psi}{\partial t}\right|_{\xi} = \left.\frac{\partial \psi}{\partial t}\right|_{x} + \left.\frac{\partial \mathbf{x}}{\partial t}\right|_{\xi} \cdot \nabla\psi = \left.\frac{\partial \psi}{\partial t}\right|_{x} + \dot{\mathbf{x}} \cdot \nabla\psi$$

$$\left.\frac{\partial \psi}{\partial t}\right|_{x} = \left.\frac{\partial \psi}{\partial t}\right|_{\xi} - \dot{\mathbf{x}} \cdot \nabla\psi$$

$$\int_{\Omega} \frac{D\psi}{Dt} w_i \mathrm{d}\Omega \approx \sum_{J} \int_{\Omega_J^{n+1}} \left(\frac{\psi_J^{n+1}(\mathbf{x}) - \psi_J^{n}(\mathbf{X})}{\Delta t} + (\mathbf{u} - \dot{\mathbf{x}}) \cdot \nabla \psi_J(\mathbf{x}) \right) w_i \mathrm{d}\Omega \quad \dot{\mathbf{x}} = \frac{\mathbf{x} - \mathbf{X}}{\Delta t}$$

- Using the closest point projection

$$\int_{\Omega} \frac{D\psi}{Dt} w_i \mathrm{d}\Omega \approx \sum_{J} \int_{\Omega_J^{n+1}} \left(\frac{\psi_J^{n+1}(\mathbf{x}) - \tilde{\psi}_J^{n}(\mathbf{x})}{\Delta t} + (\mathbf{u} - \dot{\mathbf{x}}(\mathbf{x})) \cdot \nabla \psi_J^{n+1}(\mathbf{x}) \right) w_i \mathrm{d}\Omega$$

$$\tilde{\mathbf{x}}_k^n = \begin{cases} \mathbf{x}_k, & S^n(\mathbf{x}_k) = S^{n+1}(\mathbf{x}_k) \\ P^n(\mathbf{x}_k), & S^n(\mathbf{x}_k) \neq S^{n+1}(\mathbf{x}_k) \end{cases} \quad \begin{array}{l} \tilde{\psi}_{J,k}^n = \psi_J^n(\tilde{\mathbf{x}}_k^n) \\ \tilde{\psi}_J^n(\mathbf{x}) = \sum_k \tilde{\psi}_{J,k}^n w_k \end{array} \quad \dot{\mathbf{x}}(\mathbf{x}) = \sum_k \frac{\mathbf{x}_k^{n+1} - \tilde{\mathbf{x}}_k^n}{\Delta t} w_k$$

- Recovers semi-Lagrangian in limit of $\dot{\mathbf{x}} = \mathbf{u}$